

ENGINEERING DESIGN AND COMMISSIONING PERFORMANCE OF THE ESM AND SIX SOFT X-RAY BEAMLINES AT NSLS-II*

Y. Zhu, S. O'Hara, M. Idir, E. Vescovo, I. Jarrige, S. Hulbert[†], National Synchrotron Light Source II (NSLS-II), Brookhaven National Laboratory, Upton, New York 11973, USA

Abstract

Two of the five NSLS-II Experimental Tools (NEXT) project insertion-device beamlines developed for the NSLS-II facility at Brookhaven National Laboratory are state-of-the-art soft X-ray beamlines covering the 15 eV-2300 eV photon energy range. The engineering challenges of these two beamlines included: accurate and realistic optical simulations, nearly perfect optical figure and metrology, and advanced diagnostics systems developed in-house. The measured preliminary performance (flux, spot size, resolution) of these two beamlines closely matches the calculated values. Here, the engineering design and performance measurements of these two beamlines are presented.

INTRODUCTION

The Electron Spectro-Microscopy beamline (ESM) and Soft Inelastic X-ray Scattering beamline (SIX), as part of the NEXT project funded by the Department of Energy, have recently been commissioned at NSLS-II and are now in operation.

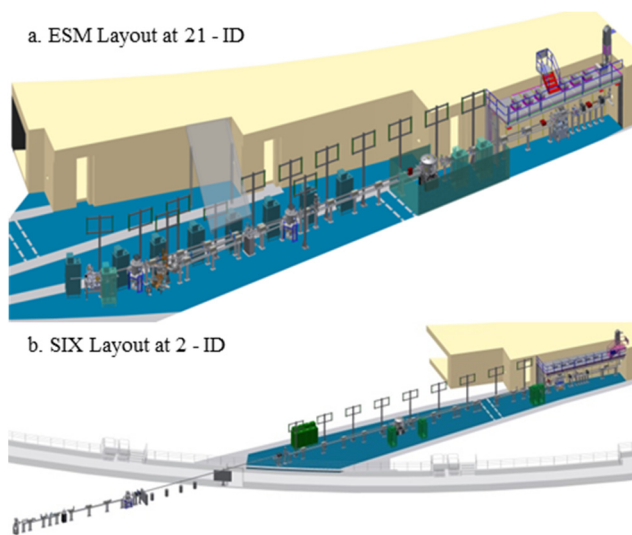


Figure 1: ESM and SIX on the NSLS-II Floor.

ESM is an insertion device beamline installed in sector 21-ID shown in Figure 1(a), a low-beta, non-extended floor space sector of the NSLS-II experimental floor. Two in-line, elliptically polarized undulators (EPU), a 2.8 m long

EPU105 and a 1.4 m long EPU57, serve as the beamline sources to cover a large photon energy range: 15 to 1500 eV. Downstream of a shared plane grating monochromator, the beam is deflected horizontally into one of two branches, the A-branch or P-branch (A for a high-resolution Angle-Resolved PhotoEmission Spectroscopy (μ -ARPES) and P for a full-field photoelectron microscopy (XPEEM)) by vertical selection of one of two identical elliptical cylinder mirrors (M3-A and M3-P).

The 105 m long SIX beamline is installed in sector 2-ID shown in Figure 1(b), a high-beta insertion device straight section feeding beam through an extended floor space sector to a satellite building. The SIX beamline covers the 180-2300 eV photon energy range by using a 3.5 m long EPU57 (upgradable to 7.0m) and is optimized to achieve a resolving power of 100,000 at 1,000 eV.

BEAMLINES OVERVIEW

ESM and SIX adopt the same type of optical scheme [1] (Figure 2; Table 1 lists beamline parameters). A horizontal internally water-cooled plane mirror (M1) serves to remove unwanted power and to separate the rest of the beamline from the Bremsstrahlung cone. The next component, a Variable Line Spacing (VLS) Plane Grating Monochromator (PGM), contains an internally water-cooled plane pre-mirror (M2) which illuminates one of four VLS gratings (300 l/mm, 600 l/mm, 800 l/mm and 1200 l/mm) for ESM and one of three VLS gratings (500 l/mm, 1200 l/mm, and 1800 l/mm) for SIX. The diffracted beam from the gratings is focused, vertically by the VLS grating and horizontally by an elliptical cylinder mirror (M3), at a plane occupied by high precision horizontal and vertical slits which define the energy resolution (vertical) and serve as a secondary source. A refocused image of the secondary source is produced at the sample position by either an ellipsoidal mirror (M4, at SIX and ESM B-branch) or by a KB mirror pair (ESM A).

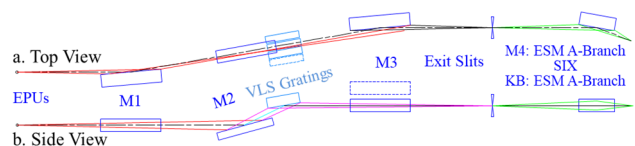


Figure 2: ESM and SIX optical schemes. The dashed rectangles represent the 4th ESM grating and the 2nd ESM M3 mirror.

* Work supported by the U. S. Department of Energy under Contract No. DE-SC0012704.

[†] Hulbert@bnl.gov

Content from this work may be used under the terms of the CC BY 3.0 licence (© 2018). Any distribution of this work must maintain attribution to the author(s), title of the work, publisher, and DOI.

Table 1: ESM and SIX Parameters

| | ESM | SIX |
|----------------------------|---|--|
| Source | EPU105, EPU57 | EPU57 |
| Energy Range | 15 - 200 eV, 200 - 1500 eV | 180 - 2300 eV |
| Resolution (ΔE) | ~ 1 meV up to 100 eV ~ 100 meV up to 1000 eV | ~ 10 meV at 1,000 eV |
| Flux | μ -ARPES: 10^{10} - 10^{11} photons/second XPEEM: 10^{11} - 10^{12} photons/second | 10^{11} - 10^{12} photons/second |
| Beam Size at sample (FWHM) | μ -ARPES: ≤ 1 μ m, XPEEM: ≤ 40 μ m | 6 μ m (horizontal) \times 0.6 μ m (vertical) |

ENGINEERING DESIGN AND IMPLEMENTATION

The engineering challenges presented by the ESM and SIX beamlines included: optics optimization and metrology, high heat load optics cooling solutions, and advanced diagnostics system design for beamline commissioning and operation. Engineering standardization and modularization activities were implemented for the engineering design and implementation of both beamlines. All corresponding components of ESM and SIX share one engineering solution, with detailed parameter values that are dedicatedly optimized for each beamline.

Here, the ESM engineering design and implementation is presented as an example to elaborate the engineering design process for both ESM and SIX.

Optics Engineering Design and Metrology

Conventional ray trace software XOP SHADOWVUI [2] was used to perform extensive ray trace simulations to optimize the ESM and SIX optical configurations and parameters. In total, the ESM and SIX beamline optics consist of 11 Au-coated (50 nm thickness) mirrors and 7 VLS gratings. The surface figure of these optics is state-of-the-art in order to maintain the brightness of source photon beams and to achieve the target energy resolution and spot size values at the sample positions. Table 2 shows the optimized optical parameters for the ESM mirrors.

All optical elements were measured in the NSLS-II optical metrology lab using state-of-the-art surface figure measurement tools such as Stitching Shack-Hartman (SSH) [3] and Nano Surface Profiler (NSP) [4]. Figure 3 shows SSH metrology results for a typical focusing mirror (M3) for the ESM beamline.

Table 2: ESM Mirrors Optimized Parameters

| Optics | M1 | M2 | μ -ARPES-Branch | | | XPEEM-Branch | |
|--|-----------------|-----------------|---------------------|---------------------|-----------------|-----------------|-----------------|
| | | | M3-A | KB-H | KB-V | M3-A | M4-P |
| Object distance (m) | - | - | 51.5 | 6.6 | 6.925 | 51.5 | 9 |
| Image distance (m) | - | - | 3.5 | 0.7 | 0.375 | 3.5 | 3 |
| Grazing angle ($^\circ$) | 1.25 | 2.2-15.5 | 1.5 | 2.5 | 2.5 | 1.5 | 2.5 |
| Deflection Direction | Inboard | Upward | Outboard | | Upward | Inboard | |
| Mirror shape | Plane | Plane | | Elliptical Cylinder | | | Ellipsoid |
| Optical active area (L(mm) \times W(mm)) | 535 \times 16 | 515 \times 22 | 600 \times 15 | 335 \times 15 | 300 \times 10 | 600 \times 15 | 600 \times 15 |
| Longitudinal RMS slope error (μ rad) | | < 0.2 | | < 0.1 | | | < 0.5 |

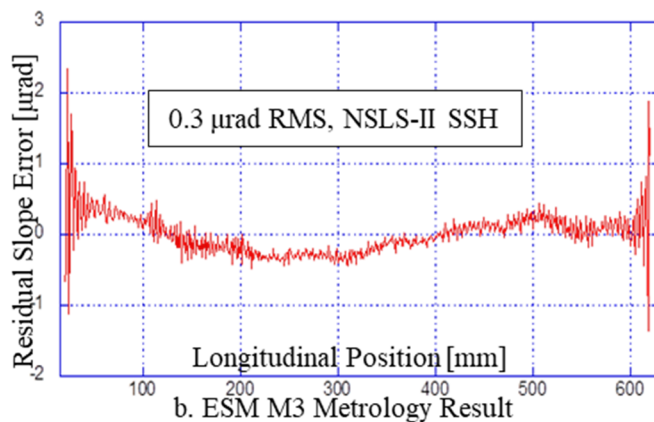
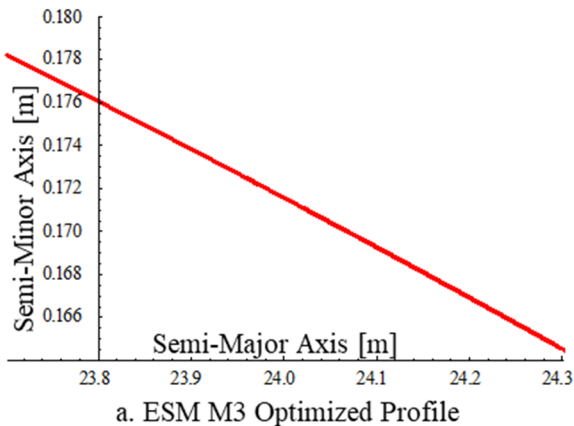


Figure 3: ESM M3-A mirror: optimized surface figure and metrology results. The residual slope error of this horizontally-focusing mirror is 0.3 μ rad RMS, less than the specified value of 0.5 μ rad.

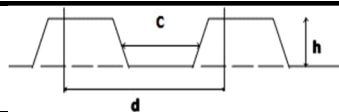
Four laminar VLS gratings are employed at ESM to cover the full 15 – 1500 eV energy range and for different applications. They are: one low energy grating (LEG, 800 l/mm), one medium energy grating (MEG, 600 l/mm), one high intensity grating (HIG, 300 l/mm), and one high energy grating (HEG, 1200 l/mm), covering the 15-100 eV, 50-200 eV, 50-300 eV, and 200-1500eV energy ranges, respectively. To optimize its diffraction efficiency over a wide energy range, the HEG grating was ruled with a sagittally-varying groove depth, ranging from 6 nm to 12 nm across the grating width. GSolver [5] software was used to optimize the grating groove parameters. After ruling, the four ESM gratings were sent to the SOLEIL optical metrology lab and metrology beamline to measure their VLS parameters, groove profiles, and diffraction efficiency. The

metrology results showed that the four gratings’ optical performance meets design requirements. Table 3 lists the optimized grating parameters and the Figure 4 shows a comparison of calculated and measured efficiency for the three fixed-groove-depth gratings.

To eliminate the distortion induced by mechanical mounting, all optics were mounted in their holders and tested as assembled units in the NSLS-II optical metrology lab. Adjustments to the clamping mechanisms were made to optimize surface figure before the optics were installed at the beamlines. Table 4 lists the surface slope errors of the four ESM gratings before and after adjustment. The results show that the grating assemblies were adjusted into the acceptable range.

Table 3: Optimized ESM Grating Parameters

| | LEG | MEG | HIG | HEG | |
|---|---|--------------------------|---------------------------|--------------------------|--------------------------|
| Energy Range (eV) | 15 - 100 | 50 - 200 | 50 - 350 | 200 - 1500 | |
| Constant C_{eff} | 3 @ 50eV | 3 @ 100eV | 2 @ 200 eV | 2 @ 900 eV | |
| Line Density | $a_0 + a_1 \times w + a_2 \times w^2 + a_3 \times w^3 + \dots$ where; w : longitudinal distance, and $w = 0$ defines the grating center. | | | | |
| | a_0 (l/mm) | 800 | 600 l/mm | 300 l/mm | 1200 l/mm |
| VLS Parameters | a_1 (l/mm ²) | 0.123453 | 0.0933142 | 0.0582427 | 0.231924 |
| | a_2 (l/mm ³) | 1.14027×10^{-5} | 8.74344×10^{-6} | 5.1248×10^{-6} | 2.05878×10^{-5} |
| | a_3 (l/mm ⁴) | 1.00155×10^{-9} | 7.84354×10^{-10} | 4.7664×10^{-10} | 1.90434×10^{-9} |
| Meridional RMS slope error (μ rad) | < 0.1 | | | | |
| Groove Depth (nm) | 48.5 | 36 | 30 | 6 - 12 | |
| Duty Cycle | 0.7 | | 0.65 | | |



Duty Cycle = $\frac{c}{d}$; (h: groove depth; c: width of groove; d: period length)

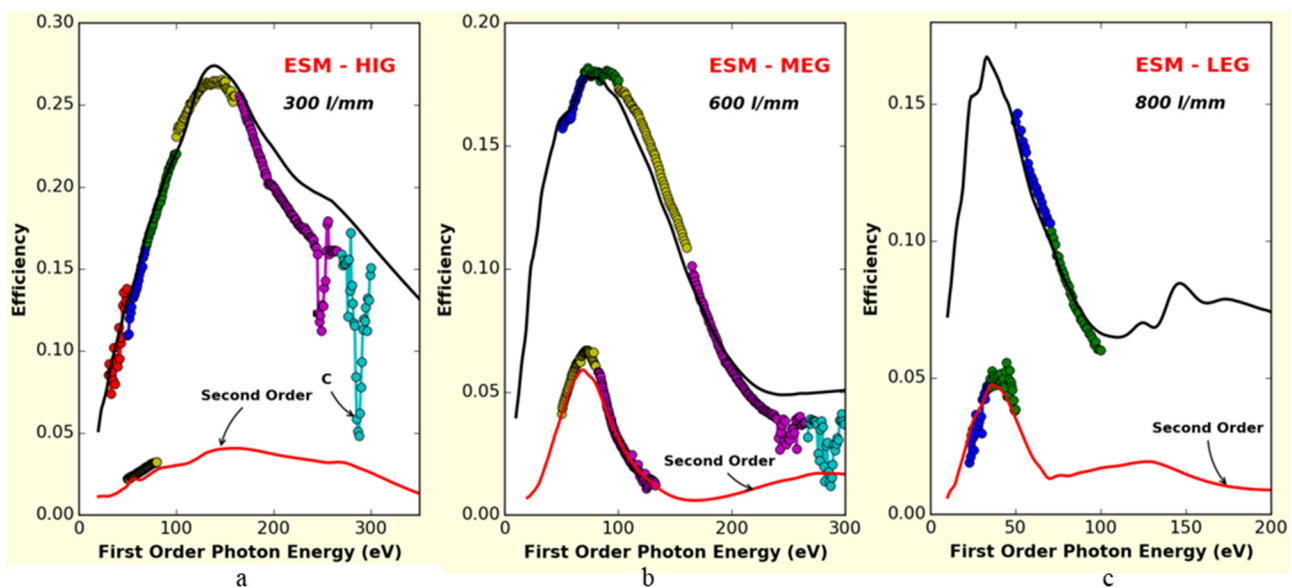


Figure 4: Calculated vs. measured efficiencies for the ESM HIG, MEG, and LEG gratings. Solid and dotted lines represent the calculated and measured efficiency, respectively.

Table 4: ESM Gratings Slope Errors (Unit: nrad)

| | | MED | HIG | LEG | HEG |
|---------------|----------|-------|------|-------|-----|
| SOLEIL (LTP) | Clamped | 259 | 195 | 180 | 150 |
| NLSL-II (SSH) | Clamped | 182.3 | 144 | - | - |
| | Adjusted | 106.2 | 85.4 | 106.4 | 101 |

Thermal Cooling Scheme

With the EPU's in the ESM and SIX beamlines operating at their highest output power setting and the NLSL-II ring current set to its maximum value (500 mA), the maximum power incident on the first optical element (M1) is more than 1.2 kW. An integral water-cooling scheme was utilized for the M1 and M2 mirrors at both ESM and SIX, while an indirect water-cooling solution was employed for all gratings. Finite element analysis (FEA) simulations were performed using ANSYS [6] to optimize the structural parameters for the M1 and M2 mirror assemblies and the grating assemblies. Figure 5 shows the power absorbed by the first three ESM optics in its low energy range.

The FEA simulations reveal that the longitudinal slope errors of the M1 and M2 mirrors and the gratings are closely linear over their useful optical areas. That is, the thermal bump shape is almost circular in all three cases. Beam performance degradation in the diffraction plane (vertical) induced by the deformation of M1 (sagittal direction) and M2 (longitudinal direction) can be corrected by tuning the VLS PGM adjustable parameter (C_{eff} [7]). The ESM M1 and M2 thermal deformation and beam vertical profile correction results at 15 eV photon energy are shown in Figures 6 and 7, respectively.

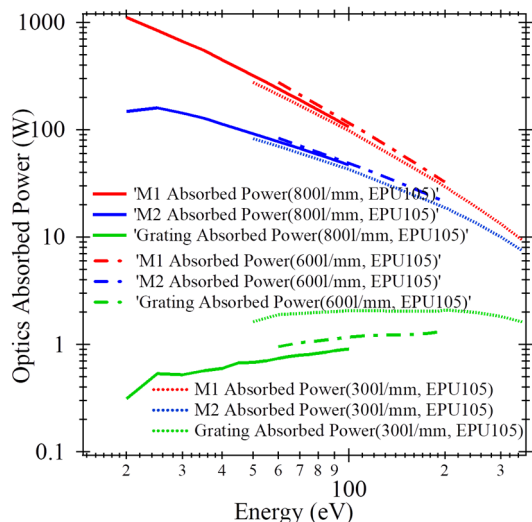


Figure 5: Power absorbed by the ESM M1 and M2 mirrors and gratings in the low energy range (15 - 300 eV). The first two mirrors (M1 and M2) and the gratings absorb 1.1 kW, 159 W, and 1.1 W of worst-case power, respectively.

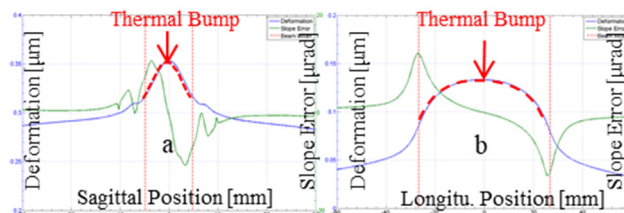


Figure 6: ESM M1 and M2 optical surface deformation: (a) The sagittal radius of curvature of ESM M1 is 461 m and slope error is $< 1 \mu\text{rad}$; (b) The tangential radius of curvature of ESM M2 is 7.4 km and slope error is $< 1 \mu\text{rad}$.

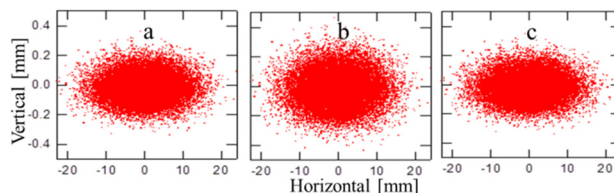


Figure 7: ESM beam spot at the exit slit plane, at 15 eV photon energy: (a) without heat load, $C_{eff} = 2.8503$, $\sigma_{vert.} = 83.48 \mu\text{m}$, $\sigma_{horiz.} = 6.0206 \text{ mm}$; (b) with heat load, $C_{eff} = 2.8503$, $\sigma_{vert.} = 107.02 \mu\text{m}$, $\sigma_{horiz.} = 6.0252 \text{ mm}$; (c) after correction, $C_{eff} = 2.8661$, $\sigma_{vert.} = 82.89 \mu\text{m}$, $\sigma_{horiz.} = 6.0252 \text{ mm}$.

Diagnostics Components Design

A set of beamline diagnostics instrument, developed in-house, was used to align, characterize, and monitor the beam during commissioning of the ESM and SIX beamlines. Figure 8 shows some of the types of diagnostic components installed at these beamlines.

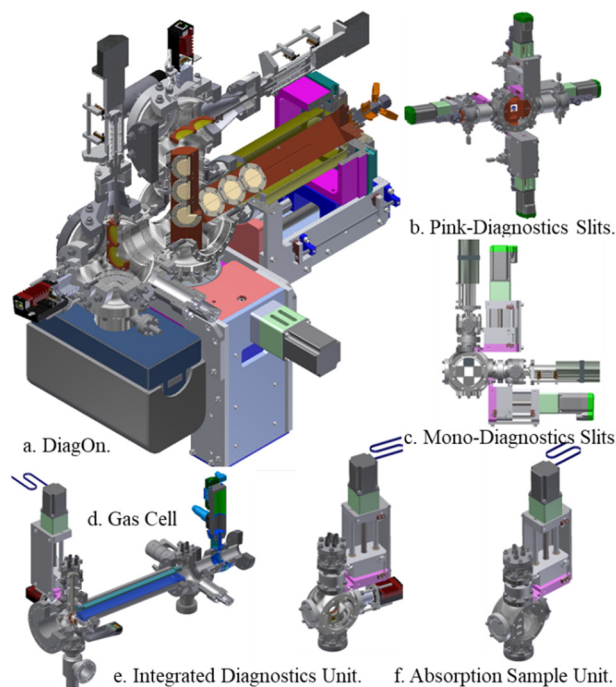


Figure 8: ESM and SIX diagnostics components: (a) DiagOn [8], first developed at SOLEIL, is used to characterize insertion device emission. NLSL-II DiagOn has ex-

Content from this work may be used under the terms of the CC BY 3.0 licence (© 2018). Any distribution of this work must maintain attribution to the author(s), title of the work, publisher, and DOI.

tended its function to provide source and beamline alignment adjustments during operation; (b), (c) Diagnostic slits, used in pink or monochromatic beam locations to trim scattered light and monitor beam position through measurement of the current drawn from the blades; (d) Gas cell, used to measure energy resolution and calibrate the beam energy; (e) Integrated diagnostics unit: one YAG crystal, one Au mesh, and one photodiode to measure the beam intensity and observe the beam profile. This unit can be also combined with the gas cell to perform energy calibration; (f) Absorption sample unit, used to calibrate beam energy, scan beam position, and measure beam intensity by measuring photo-emitted current from standard sample wires mounted in the unit.

COMMISSIONING AND PERFORMANCE

The ESM and SIX beamlines have been commissioned and operations have commenced. Preliminary test results are reported here.

The ESM and SIX EPU emission has been characterized using the NSLS-II DiagOn and the intensity diagnostic components described above. Figure 9 (a) shows the evolution of angular distribution of emission, at 2 mA ring current, from ESM EPU105 as the gap is opened from 64.2 mm to 66.8 mm, around 236 eV photon energy. The angular distributions match simulations. Figures 9(b) and 9(c) show the beam positon at different times. These images were used to align the electron beam in the storage ring. Figure 9(d) demonstrates that the DiagOn can be used at standard operating current values (320 mA shown) by scanning the upstream white beam slits when set to a small angular opening.

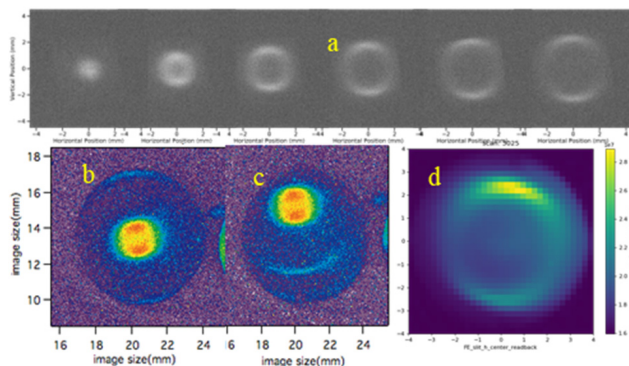


Figure 9: ESM EPU105 emission characterized using the NSLS-II DiagOn.

Figure 10 shows the ESM flux output in the low energy range (30 - 200 eV). In this figure, the black and red curves show measured flux values taken at 10 mA ring current, scaled to 500mA current, with 1 mm × 1mm and 10 mm × 10mm front end slit openings, respectively.

CONCLUSION

In conclusion, ESM and SIX have successfully accomplished commissioning, and the preliminary test results have closely achieved the calculated values.

Beamlines

Optics

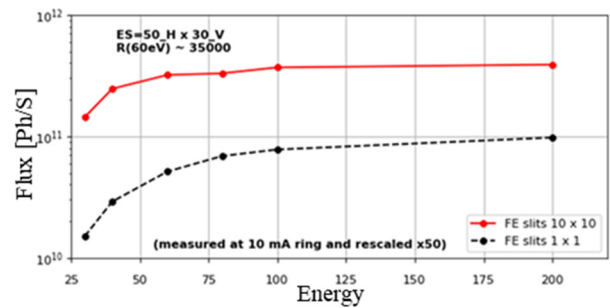


Figure 10: Measured ESM flux between 25 eV and 200 eV. The measured energy resolution at the ESM and SIX beamlines is shown in Figure 11. Figure 11(a) shows a measured energy resolution at SIX of 9 meV at 244.2 eV photon energy. Figure 10(b) shows measured energy resolution of 1.6 meV at 64.83 eV photon energy.

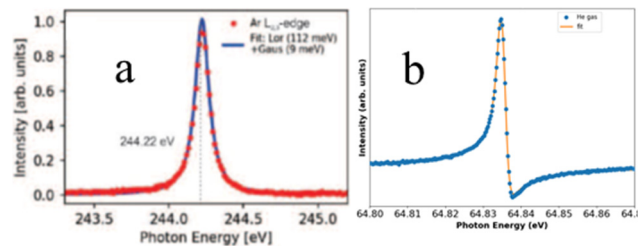


Figure 11: ESM and SIX measured energy resolution.

ACKNOWLEDEMENTS

The authors acknowledge Oleg Tchoubar and Nathalie Bouet for their support for NSLS-II DiagOn development, and the SOLEIL optical metrology group for ESM grating metrology and efficiency evaluation.

REFERENCES

- [1] R. Reininger *et al.*, “The electron spectro-microscopy beamline at National Synchrotron Light Source II: A wide photon energy range, micro-focusing beamline for photoelectron spectromicroscopies”, *Rev. Sci. Instrum.*, vol. 83(2), Feb. 2012, DOI: 10.1063/1.3681440.
- [2] Xop Shadowvui, <http://www.esrf.eu>.
- [3] M. Idir *et al.*, “A 2 D high accuracy slope measuring system based on a Stitching Shack Hartmann Optical Head”, *Optics Express*, Vol. 22, no. 3, Feb. 2014, pp. 2770-2781, DOI: 10.1364/OE.22.002770.
- [4] Qian *et al.*, “Nano-accuracy measurements and the surface profiler by use of Monolithic Hollow Penta-Prism for precision mirror testing”, *Nuclear Instruments and Methods in Physics Research Section A*, vol. 759, Sept. 2014, pp. 36–43, DOI: 10.1016/j.nima.2014.03.043.
- [5] Gsolver, <http://www.gsolver.com>.
- [6] ANSYS, <http://www.ansys.com>.
- [7] R. Reininger *et al.*, “A soft x-ray beamline capable of cancelling the performance impairment due to power absorbed on its optical elements”, *Rev. Sci. Instrum.*, vol. 79-3, Mar. 2008, DOI: 10.1063/1.2897587.
- [8] K. Desjardins *et al.*, “The DiagOn: an undulator diagnostic for SOLEIL low energy beamlines”, in *Proc. IEEE Nuclear Science Symposium Conference Record*, Dresden, Germany, Oct. 2008, pp. 2571-2574, DOI: 10.1109/NSSMIC.2008.4774883.

FROAMA05

439